

Spin-state transitions in PrCoO₃ studied with neutron powder diffractionY. Ren,¹ J.-Q. Yan,^{2,3,4} J.-S. Zhou,⁵ J. B. Goodenough,⁵ J. D. Jorgensen,⁶ S. Short,⁶ H. Kim,^{7,8} Th. Proffen,^{7,9} S. Chang,¹⁰ and R. J. McQueeney¹⁰¹*X-ray Science Division, Argonne National Laboratory, Argonne, Illinois, 60439, USA*²*Ames Laboratory, US-DOE, Ames, Iowa, 50011, USA*³*Department of Materials Science and Engineering, University of Tennessee, Knoxville, Tennessee, 37996, USA*⁴*Materials Science and Technology Division, Oak Ridge National Laboratory, Oak Ridge, Tennessee, 37831, USA*⁵*Materials Science and Engineering Program/Mechanical Engineering, University of Texas at Austin, Austin, Texas 78712, USA*⁶*Materials Science Division, Argonne National Laboratory, Argonne, Illinois, 60439, USA*⁷*Lujan Neutron Scattering Center, Los Alamos National Laboratory, Los Alamos, New Mexico, 87545, USA*⁸*Energy Technology Research Institute, National Institute of Advanced Industrial Science and Technology, Tsukuba, Ibaraki 305-8565, Japan*⁹*Neutron Scattering Science Division, Oak Ridge National Laboratory, Oak Ridge, Tennessee, 37831, USA*¹⁰*Ames Laboratory and Department of Physics and Astronomy, Iowa State University, Ames, Iowa, 50011, USA*

(Received 13 October 2011; revised manuscript received 6 November 2011; published 5 December 2011)

The crystal structure of PrCoO₃ has been studied with high-resolution neutron powder diffraction and pair-distribution-function analysis in the temperature range from 12–600 K. The compound has the orthorhombic (*Pbnm*) perovskite structure over the entire temperature range. The temperature dependence of the average Co-O bond length shows clear anomalies near 60 K and 200 K where anomalous temperature dependencies of thermal conductivity and magnetic susceptibility have been reported. The data show a constant intermediate-spin-state fraction within 60 < *T* < 200 K and excitation of high-spin-state Co(III) above 200 K.

DOI: [10.1103/PhysRevB.84.214409](https://doi.org/10.1103/PhysRevB.84.214409)

PACS number(s): 71.70.Ej, 61.05.fm, 61.50.Ks, 68.18.Jk

I. INTRODUCTION

The peculiar magnetic and transport properties associated with the spin-state transition in LaCoO₃ have been continuously attracting much attention since the 1950s.^{1–8} Whether and where thermal excitation from a low-spin state to a high-spin state in an octahedral site passes through an intermediate-spin state is a question of general interest. Its bulk ground state is a diamagnetic insulator. With increasing temperature, the magnetic susceptibility increases sharply above ~35 K and reaches a maximum near 100 K followed by a more gradual increase of higher-spin-state ions. Above 500 K, there is a smooth transition from an insulator to a more conducting phase. Early publications generally followed the Co(III) LS (low spin, t^6e^0 , $S = 0$) to HS (high spin, t^4e^2 , $S = 2$) scenario based on Goodenough's original model.¹ In 1995, Potze *et al.*³ proposed a LS to IS (intermediate spin, t^5e^1 , $S = 1$) to HS three-spin-state model with increasing temperature. The IS Co(III) ions are Jahn-Teller (JT) active whereas the HS Co(III) is a weak JT ion. Although the LS-IS-HS model has been widely used to explain various experimental data, the precise picture of the spin state as a function of temperature is still under hot debate. Evidences for the IS state include optical spectroscopy,⁹ electron energy-loss spectroscopy,¹⁰ and neutron analysis.^{11,12} These findings indicate that an IS state could be stabilized by local dynamic JT site distortions. Whereas a magnetic phase has been found to be associated with the surface state,^{5,13} and a strain-induced state,¹⁴ these methods provide no distinction between the IS and HS spin state on Co(III) ions. A structural determination by diffraction methods can be used to identify a static IS versus a HS state; but no conclusion with regard to this question was made in the previous neutron diffraction studies.^{15–17} This failure could be attributed to: (a) The rhombohedral $R\bar{3}c$ symmetry of LaCoO₃ allows only a single Co-O bond length, which rules

out the possibility of a long-range orbital ordering, and (b) the population of the Co(III) with the IS spin state is too low for a globally cooperative JT distortion. On the other hand, Maris *et al.*¹⁸ concluded, based on a high-resolution x-ray diffraction study, that the symmetry was lowered to be monoclinic. A continuous increase of site distortion as temperature increases is not compatible with the population change proposed in the LS-IS-HS model. In order to fully explore all possible spin-state transitions without the symmetry restriction of LaCoO₃, we chose to study a similar compound, PrCoO₃, with the *Pbnm* symmetry that is compatible with either a dynamic or a cooperative Jahn-Teller (JT) distortion. Radaelli and Cheong¹⁷ pointed out that the significant structural disorder due to a coexistence of different spin states should be evident in the atomic displacement parameters. Unfortunately, they could not support this argument within the accuracy of their neutron diffraction study of LaCoO₃. However, the subtle correlation between the spin-state transition and the lattice dynamics is picked up sensitively by the thermal conductivity $\kappa(T)$ measurements of RCoO₃.¹⁹ Although the anomaly of κ at about 35 K in LaCoO₃ corresponds well to the spin-state transition, it was a puzzle to assign two anomalies of κ at about 60 K and 200 K found in PrCoO₃.

Whereas the LS state is stabilized at $T < 35$ K in LaCoO₃, the substitution of La by smaller rare-earth ions R³⁺ not only converts the structure from the rhombohedral $R\bar{3}c$ to the orthorhombic *Pbnm*, but narrows the σ^* bandwidth so as to stabilize the LS state of the Co(III) ions to higher temperatures.²⁰ The narrow temperature range where the IS state could be possibly observed, may be squeezed out as the transition from the LS state to a higher spin state moves to higher temperatures in the RCoO₃ with smaller R³⁺. Having the *Pbnm* space group and exhibiting two anomalies of κ below room temperature, PrCoO₃ may be a unique system

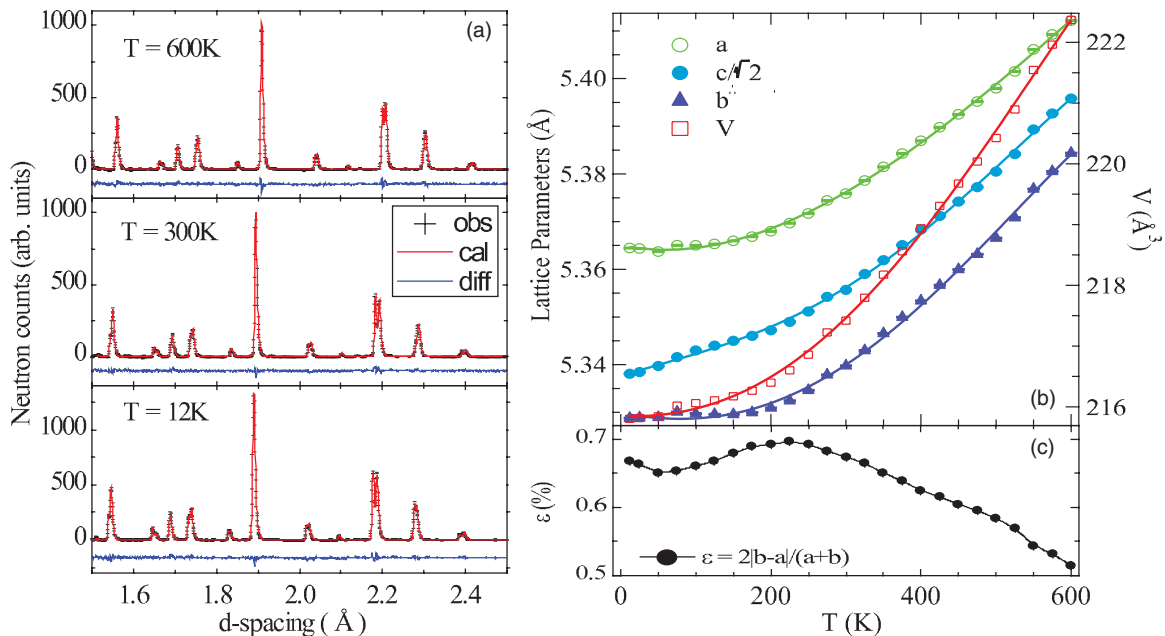


FIG. 1. (Color online) (a) Sections of neutron diffraction patterns and best fits of PrCoO₃. Temperature dependence of (b) lattice parameters and unit cell volume, and (c) lattice strain ϵ .

for the study of spin-state transitions in the perovskite RCoO₃ family. Here we report a thorough structural study of PrCoO₃ by neutron powder diffraction in the temperature range 12 K < T < 600 K. The comparison between the result of this study and the structural data of LaCoO₃ in the literature not only clarifies the origin of the anomalies of $\kappa(T)$ found in PrCoO₃, but confirms a one-step LS to HS transition in rhombohedral LaCoO₃.

II. EXPERIMENTAL DETAILS

The PrCoO₃ powder sample was obtained by pulverizing single crystals grown by the floating-zone method. Crystals grown under the same condition have been used in the physical properties measurements.^{5,19,20} High-resolution neutron powder diffraction measurements were performed from 12–600 K using the special environment powder diffractometer (SEPD) at the Intense Pulsed Neutron Source (IPNS), Argonne National Laboratory.²¹ Structural refinements were carried out using the GSAS program with the EXPGUI interface,²² in which isotropic thermal parameters (U_{iso}) of Co and Pr and anisotropic thermal parameters (U_{aniso}) for oxygen were used. The refinement with U_{aniso} for oxygen was found to improve significantly the fitting agreement (an improvement of more than 8% at high temperatures), indicating the importance of the anisotropic thermal motions. The final average R factor is $R_{wp} = 4.5\%$ with an average $\chi^2 \sim 1.4$.

High-quality neutron diffraction data for pair-distribution-function (PDF) analysis were collected at some characteristic temperatures from 15–300 K using the high-resolution neutron powder diffractometer (NPDF) at the Lujan Neutron Scattering Center, Los Alamos National Laboratory.²³ The total scattering structure function $S(Q)$, and the corresponding PDF, $G(r)$, as well as the pair-density-function, $\rho(r)$, for each run were obtained by using the software PDFgetN.²⁴ The data processing

includes corrections for detector dead time and efficiency, background, absorption, multiple scattering, and inelastic effects, and normalization by the incident flux and the total sample scattering cross section.

III. RESULTS AND DISCUSSION

In the whole temperature range of this study, PrCoO₃ remains orthorhombic with the $Pbnm$ space group and no long-range magnetic ordering was detected [Fig. 1(a)]. The temperature dependence of the lattice parameters and unit-cell volume of PrCoO₃ are shown in Fig. 1(b). Below 200 K, the a and b axes are almost temperature independent while the c axis shows a finite temperature dependence. Figure 1(c) shows the temperature dependence of the lattice orthorhombic strain, defined by $\epsilon = 2|b - a|/(a + b)$, which clearly indicates structural anomalies at about 60 K, 200 K, and 525 K.

Figure 2 shows the temperature dependence of the Co-O bond lengths. In the model with isotropic thermal motions for oxygen atoms, the CoO₆ octahedra are slightly compressed along the c axis at low temperature. With increasing temperature, the two pairs of longer Co-O2 bonds in the a - b plane start to split into long and short pairs with the Co-O1 bond along the c axis becoming intermediate to the two a - b -plane bonds above ~ 225 K. The difference between the long and the short bonds in the a - b plane becomes larger with increasing temperature. The fittings with the isotropic thermal parameters give rise to an apparent distortion of the Co bonding environment. However, the fittings with the anisotropic thermal parameters for oxygen atoms show that these distortions become smaller. The Co-O1 bond lengths along the c axis are not affected by the two models.

We discuss two implications of these structural data:

(i) *Temperature dependence of the lattice parameters.* For ABO₃ perovskites with the $Pbnm$ symmetry, the corner-shared

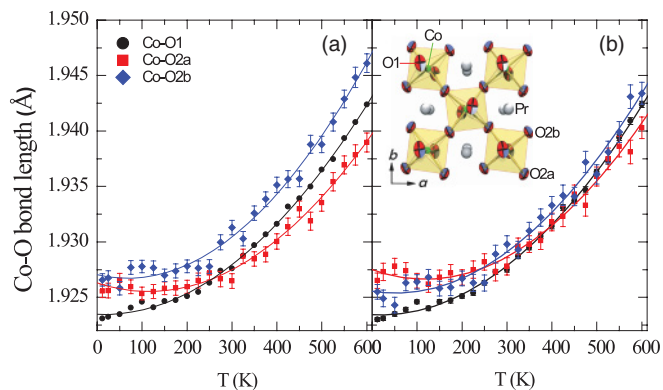


FIG. 2. (Color online) Temperature dependence of the Co-O bond lengths for PrCoO₃, as obtained from GSAS fits to the neutron diffraction data with (a) isotropic thermal parameters and (b) with anisotropic thermal parameters for the oxygen atoms. The inset shows crystal structure with anisotropic thermal parameters for oxygen. O1 is the oxygen atom at the 4c site, and O2a and O2b are the oxygen atoms at 8d sites.

BO₆ octahedra involve two fixed rotation axes, the [001] and [110] directions of the cubic unit cell, described by the $a^-a^-b^+$ tilting system in Glazer notation. A $b > a$ is always resolved for the structure provided that the BO₆ octahedra are rigid. However, an octahedral-site distortion that reduces the O2a-B-O2b bond angle (open along the a axis) from 90° leads to a collapse of $b - a$ and eventually to an $a > b$. The orthorhombic perovskite phase with an $a > b$ is always found to be the precursor of a phase transition to the rhombohedral phase with $R\bar{3}c$ symmetry as the tolerance factor $t \equiv (A - O)/[\sqrt{2}(B - O)]$ increases. This structural rule has been demonstrated for the RM³⁺O₃ perovskites where R is a rare-earth metal and M is a transition metal.²⁵ The structural change from the orthorhombic PrCoO₃ with $a > b$ to the rhombohedral LaCoO₃ matches the rule well. On the other hand, the t factor increases as temperature rises since the thermal expansion of the R-O bond is larger than that of the M-O bond for almost all RMO₃ perovskites. The t factor increase with temperature is a driving force for the orthorhombic LaGaO₃ perovskite with $a > b$ at room temperature to undergo an orthorhombic-rhombohedral phase transition at $T \approx 413$ K.²⁶ The PrCoO₃ perovskite has $a > b$ at room temperature, which is similar to LaGaO₃. In sharp contrast to LaGaO₃, however, PrCoO₃ remains orthorhombic up to 600 K and $a - b$ decreases at higher temperatures as shown in Fig. 1(c), which indicates that the thermal expansion of the Co-O bond is larger than that of the Pr-O bond. This behavior was also observed by Knizek.²⁷ By using the thermal expansion of the R-O bond as a reference, we are able in this comparative study to demonstrate unambiguously an unusually large thermal expansion of the Co-O bond in PrCoO₃ due to an increase in the IS or HS population as temperature increases. This qualitative conclusion will be further proven in the following by a quantitative study of the Co-O bond length as resolved by Rietveld refinements.

(ii) *Characterization of the spin state of a Co(III) ion in terms of the Co-O bond length and its thermal expansion.* The LS(t^6e^0) state is JT inactive, the IS(t^5e^1) is JT active and

the HS(t^4e^2) may have a weak JT distortion. An isolated IS state in a matrix of LS states may induce only an extremely weak octahedral-site distortion. Therefore, the transition to a higher spin state might be better monitored by a precision measurement of the volume change of the CoO₆ octahedra. As shown in Fig. 2(b), the long Co-O bond calculated by using the anisotropic U parameter could switch from along the a axis to along the b as temperature varies, which matches the intrinsic character of the $Pbnm$ orthorhombic structure. However, the average Co-O bond length, which is related to the volume of CoO₆ octahedra, is insensitive to the choice of the isotropic or anisotropic U parameters. The average M-O bond length is also not sensitive to the change of M-O-M bond angle and the magnitude of any JT distortion as shown by RMnO₃²⁸ and by RFeO₃.²⁹ In the RCoO₃ perovskites, the introduction of antibonding σ -bond e orbitals with high-spin occupation is a major factor to increase the average Co-O bond length.

We plot in Fig. 3(a) the temperature dependence of the $\langle M-O \rangle$ bond length of PrCoO₃, LaCoO₃, PrCrO₃ and PrGaO₃. The $\langle Ga-O \rangle$ of PrGaO₃ is selected as an example to show the regular thermal expansion of an $\langle M-O \rangle$ bond since the Ga³⁺ ion has no spin or orbital change. The thermal expansion of the $\langle Ga-O \rangle$ bond obtained from PrGaO₃ appears to be universal for other RMO₃ perovskites as is seen by superimposing the temperature dependence of $\langle Cr-O \rangle$ in PrCrO₃ for temperatures at $T > T_N$ and $T < T_N$. A bond length reduction at T_N in PrCrO₃ can be well attributed to the exchange restriction in this type-G antiferromagnet. LaCoO₃ clearly has the LS state dominating at $T < 35$ K. Although PrCoO₃ shows slightly distorted CoO₆ octahedra at low temperatures, the $\langle Co-O \rangle \approx 1.925$ Å for the LS state obtained from LaCoO₃ is nearly identical with the LS $\langle Co-O \rangle$ of PrCoO₃ in Fig. 3(a). This observation further justifies that the $\langle M-O \rangle$ bond length is insensitive to the structural distortion. On the high-temperature side of Fig. 3(a), it is also widely believed that the HS state is dominant at $T > 300$ K in LaCoO₃. Therefore, the phase with a continuous increase of the HS state population is characterized by an anomalously large $\langle Co-O \rangle$ bond thermal expansion, which is larger by factor four than that of a regular $\langle M-O \rangle$ bond such as $\langle Ga-O \rangle$ in PrGaO₃. This criterion for excitation to the HS state drawn from LaCoO₃ is nearly perfectly fulfilled for PrCoO₃ at $T > 300$ K as is also shown in Fig. 3(a).

The curve of $\langle Co-O \rangle$ versus T in Fig. 3(a) shows a jump at about 60 K followed by a state having a very small, negative thermal expansion of the bond over the temperature range 60–200 K. Moreover, within that same temperature range, the magnetic susceptibility follows very closely a Curie-Weiss law, Fig. 3(b). At nearly the same temperature where the $\langle Co-O \rangle$ bond length jumps, the thermal conductivity κ collapses. It is clear that a small amount of the magnetic Co(III) ions are created starting a little below 60 K and that the concentration of the magnetic ions, about 0.3 IS Co(III)/Co derived from a Curie-Weiss fitting, remains constant in the temperature range from 60–200 K. Both the IS and HS states of the Co(III) ion are magnetic. However, the following considerations make the HS state unlikely in this temperature range: a) the perovskite phase with the HS state is characterized by a continuous increase of the HS Co(III) population with increasing temperature once the HS Co(III) ions are created, which is well demonstrated

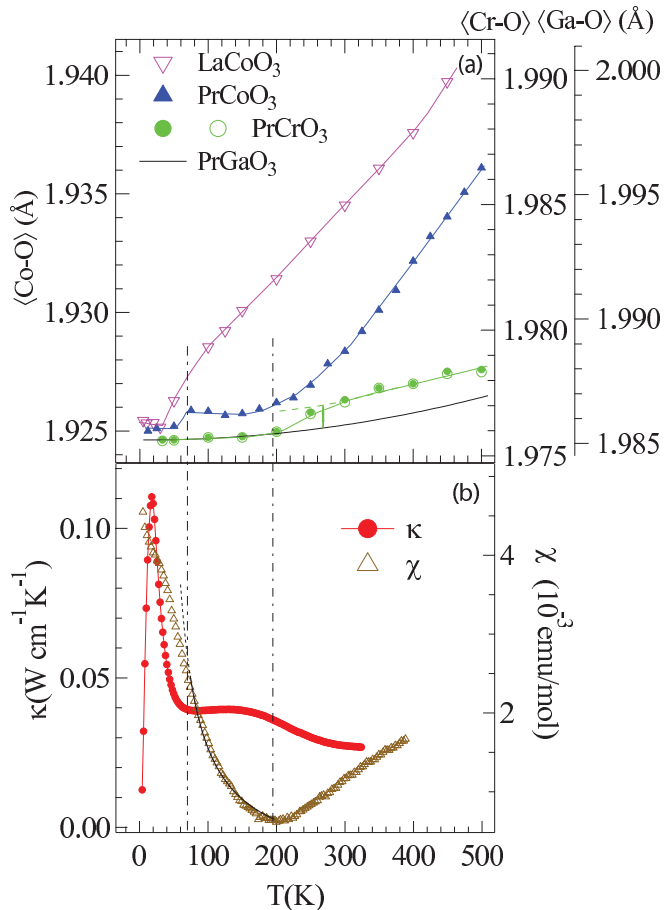


FIG. 3. (Color online) (a) Temperature dependence of the $\langle M-O \rangle$ for LaCoO_3 , PrCoO_3 , PrGaO_3 , and PrCrO_3 ; the solid and open circles are for the $\langle \text{Cr-O} \rangle$ resolved with the $U(\text{O})_{\text{aniso}}$ and $U(\text{O})_{\text{iso}}$, respectively; the $\langle \text{Co-O} \rangle$ is from refinements with the U_{aniso} ; the data of LaCoO_3 and PrGaO_3 are from Ref. 30. The windows of the vertical scale in this plot are set for $\langle \text{Co-O} \rangle$, $\langle \text{Cr-O} \rangle$, and $\langle \text{Ga-O} \rangle$ to have an identical range of $\Delta \langle M-O \rangle / \langle M-O \rangle$. (b) temperature dependencies of thermal conductivity κ and magnetic susceptibility χ . The paramagnetic contribution from Pr^{3+} , which was obtained from the isostructural PrAlO_3 perovskite, has been subtracted from the $\chi(T)$ of PrCoO_3 . Thermal conductivity and magnetic susceptibility data are from Ref. 19.

in LaCoO_3 and PrCoO_3 at high temperatures; b) although the concentration of magnetic Co(III) ions in the phase within 60–200 K is low relative to the HS Co(III) ions at high temperature, the average octahedral-site distortion obtained from the Co-O bond lengths of Fig. 2(b) in the temperature range 60–200 K is much higher than that at high temperatures. The LS Co-O bond may have a negative thermal expansion as seen more clearly in LaCoO_3 below 35 K. With a constant, low IS population, the matrix with dominant LS Co(III) is responsible for the slight negative thermal expansion observed in PrCoO_3 within the temperature range from 60–200 K. In orthorhombic PrCoO_3 , the split between $x^2 - y^2$ and $3z^2 - r^2$ orbitals of α spin certainly enhances the possibility that only one of them is occupied during the thermally driven spin-state transition. Moreover, the negative thermal expansion as seen in $\langle \text{Co-O} \rangle$ versus T of the IS state would shift the

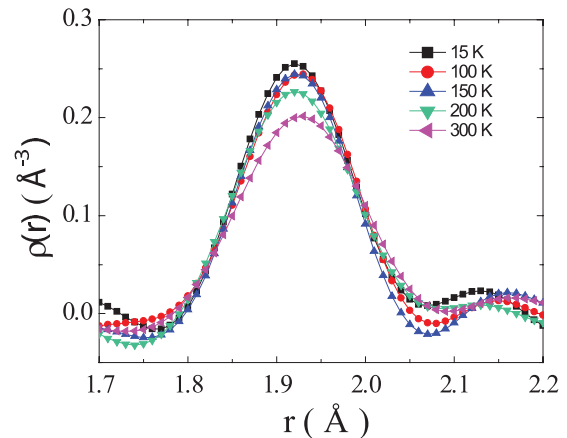


FIG. 4. (Color online) Sections of the PDF, obtained with $Q_{\text{max}} = 35 \text{ \AA}^{-1}$, showing the Co-O bond length at different temperatures.

onset of IS states to higher temperature as the temperature increases. The complete characterization of the temperature dependence of $\langle \text{Co-O} \rangle$ of PrCoO_3 and the comparison with that of LaCoO_3 in turn support that the LS-HS model is applicable in rhombohedral LaCoO_3 as originally suggested by Goodenough.¹

In Fig. 4, we plot the observed pair-density-function, $\rho(r)$, for several characteristic temperatures, which shows the region for the Co-O pairs. The average peak position has little change from 100–200K, and there is no peak splitting, which is different from the result observed in LaCoO_3 by Louca *et al.*¹² However, our result agrees with most recent reports by Sundaram *et al.*⁷ and by Yu *et al.*,³¹ which suggests little fraction of IS Co(III) exhibiting a large static JT distortion in the nonmagnetic LS Co(III) matrix.

IV. CONCLUSION

In conclusion, although there is no cooperative JT distortion in the temperature range 12–600 K, the octahedral volume change as a function of temperature reveals a remarkable correlation to the spin-state transition. At low temperatures, the bond length $\langle \text{Co-O} \rangle$ of LaCoO_3 and PrCoO_3 converges to $\sim 1.925 \text{ \AA}$ in the LS state. At $T > 300 \text{ K}$, the HS state in LaCoO_3 and PrCoO_3 is characterized by a very large thermal expansion of the $\langle \text{Co-O} \rangle$ bond. A constant, small fraction of IS-state Co(III) has been identified in PrCoO_3 within the temperature range $60 < T < 200 \text{ K}$. Although there is no direct observation of the split peak in PDF data, the onset temperatures for the IS state and HS state as deduced from the $\langle \text{Co-O} \rangle$ versus T curve correspond very well to temperatures where thermal conductivity is anomalously suppressed as temperature increases. Features of the IS state in the curves of $\langle \text{Co-O} \rangle$ versus T and $\kappa(T)$ are clearly missed in rhombohedral LaCoO_3 , which confirms the LS-HS model in LaCoO_3 as originally suggested by Goodenough.

ACKNOWLEDGMENTS

Work at Argonne National Laboratory is supported by the US Department of Energy, Division of Basic Energy Science, under Contract No. DE-AC02-06CH11357. Work

at ORNL is supported by the US Department of Energy, Basic Energy Sciences, Materials Science and Engineering Division. Ames Laboratory is operated for the US Department of Energy by Iowa State University under Contract No. DE-AC02-07CH11358. J.S.Z. and J.B.G. thank the NSF (DMR 0904282, DMR 1122603) and the Robert A Welch foundation

(Grant F-1066) for support. This work has benefitted from the use of the NPDF beamline at the Lujan Center at Los Alamos Neutron Science Center, funded by the US DOE, Office of Basic Energy Sciences. Los Alamos National Laboratory is operated by Los Alamos National Security LLC under DOE Contract No. DE-AC52-06NA25396.

-
- ¹J. B. Goodenough, *J. Phys. Chem. Solids* **6**, 287 (1958).
²K. Asai, O. Yokokura, N. Nishimori, H. Chou, J. M. Tranquada, G. Shirane, S. Higuchi, Y. Okajima, and K. Kohn, *Phys. Rev. B* **50**, 3025 (1994).
³R. H. Potze, G. A. Sawatzky, and M. Abbate, *Phys. Rev. B* **51**, 11501 (1995).
⁴M. A. Korotin, S. Yu. Ezhov, I. V. Solovyev, V. I. Anisimov, D. I. Khomskii, and G. A. Sawatzky, *Phys. Rev. B* **54**, 5309 (1996).
⁵J.-Q. Yan, J.-S. Zhou, and J. B. Goodenough, *Phys. Rev. B* **70**, 014402 (2004).
⁶J. Baier, S. Jodlauk, M. Kriener, A. Reichl, C. Zobel, H. Kierspel, A. Freimuth, and T. Lorenz, *Phys. Rev. B* **71**, 014443 (2005).
⁷N. Sundaram, Y. Jiang, I. E. Anderson, D. P. Belanger, C. H. Booth, F. Bridges, J. F. Mitchell, Th. Proffen, and H. Zheng, *Phys. Rev. Lett.* **102**, 026401 (2009).
⁸D. Phelan, D. Louca, S. Rosenkranz, S.-H. Lee, Y. Qiu, P. J. Chupas, R. Osborn, H. Zheng, J. F. Mitchell, J. R. D. Copley, J. L. Sarrao, and Y. Moritomo, *Phys. Rev. Lett.* **96**, 027201 (2006).
⁹S. Yamaguchi, Y. Okimoto, and Y. Tokura, *Phys. Rev. B* **55**, R8666 (1997).
¹⁰R. F. Klie, J. C. Zheng and Y. Zhu, M. Varela, J. Wu, and C. Leighton, *Phys. Rev. Lett.* **99**, 47203 (2007).
¹¹D. Louca and J. L. Sarrao, *Phys. Rev. Lett.* **91**, 155501 (2003).
¹²D. Louca, J. L. Sarrao, J. D. Thompson, H. Röder, and G. H. Kwei, *Phys. Rev. B* **60**, 10378 (1999).
¹³A. Harada, T. Taniyama, Y. Takeuchi, T. Sato, T. Kyômen, and M. Itoh, *Phys. Rev. B* **75**, 184426 (2007).
¹⁴D. Fuchs, C. Pinta, T. Schwarz, P. Schweiss, P. Nagel, S. Schuppler, R. Schneider, M. Merz, G. Roth, and H. v. Löhneysen, *Phys. Rev. B* **75**, 144402 (2007).
¹⁵G. Thornton, B. C. Tofield, and A. W. Hewat, *J. Solid State Chem.* **61**, 301 (1986).
¹⁶S. Xu, Y. Moritomo, K. Mori, T. Kamiyama, T. Saitoh, and A. Nakamura, *J. Phys. Soc. Jpn.* **70**, 3296 (2001).
¹⁷P. G. Radaelli and S.-W. Cheong, *Phys. Rev. B* **66**, 094408 (2002).
¹⁸G. Maris, Y. Ren, V. Volotchaev, C. Zobel, T. Lorenz, and T. T. M. Palstra, *Phys. Rev. B* **67**, 224423 (2003).
¹⁹J.-Q. Yan, J.-S. Zhou, and J. B. Goodenough, *Phys. Rev. B* **69**, 134409 (2004).
²⁰J.-S. Zhou, J.-Q. Yan, and J. B. Goodenough, *Phys. Rev. B* **71**, 220103(R) (2005).
²¹J. D. Jorgensen, J. Faber Jr., J. M. Carpenter, R. K. Crawford, J. R. Haumann, R. L. Hitterman, R. Kleb, G. E. Ostrowsku, F. J. Rotella, and T. G. Worlton, *J. Appl. Cryst.* **22**, 321 (1989).
²²A. C. Larson and R. B. Von Dreele, Los Alamos National Laboratory Report, LAUR. 86-748 (2004); B. H. Toby, *J. Appl. Cryst.* **34**, 210 (2001).
²³Th. Proffen, T. Egami, S. J. L. Billinge, A. K. Cheetham, D. Louca, and J. B. Parise, *Appl. Phys. A* **74**, S163 (2002).
²⁴P. F. Peterson, M. Gutmann, Th. Proffen, and S. J. L. Billinge, *J. Appl. Crystallogr.* **33**, 1192 (2000).
²⁵J.-S. Zhou and J. B. Goodenough, *Phys. Rev. Lett.* **94**, 065501 (2005).
²⁶W. Marti, P. Fischer, F. Altorfer, H. J. Scheel, and M. Tadin, *J. Phys. Condens. Matter* **6**, 127 (1994).
²⁷K. Knížek, J. Hejtmánek, Z. Jiráček, P. Tomeš, P. Henry, and G. André, *Phys. Rev. B* **79**, 134103 (2009).
²⁸J.-S. Zhou and J. B. Goodenough, *Phys. Rev. Lett.* **96**, 247202 (2006).
²⁹M. Marezio, J. P. Remeika, and P. D. Dernier, *Acta Crystallogr. B* **26**, 2008 (1970).
³⁰L. Vasylechko, Ye. Pivak, A. Senyshyn, D. Savvitskii, M. Berkowski, H. Borrmann, M. Knapp, and C. Paulmann, *J. Solid State Chem.* **178**, 270 (2005).
³¹J. Yu, D. Phelan, and D. Louca, *Phys. Rev. B* **84**, 132410 (2011).